Transport properties of carriers in GaAs obtained using the photoacoustic method with the transmission detection configuration

1996 J. Phys.: Condens. Matter 8 5673

(http://iopscience.iop.org/0953-8984/8/30/016)

J. Phys.: Condens. Matter **8** (1996) 5673–5683. Printed in the UK

Transport properties of carriers in GaAs obtained using the photoacoustic method with the transmission detection configuration

P M Nikolić†, D M Todorović†, A I Bojičić†, K T Radulović†, D Urošević‡, J Elazar§, V Blagojević†, P Mihajlović† and M Miletić†

† Joint Laboratory for Advanced Materials of SASA, Knez Mihailova 35/4, 11000 Belgrade, PO Box 745, Yugoslavia

‡ Mathematical Institute of SASA, Knez Mihailova 35/4, 11000 Belgrade, Yugoslavia

§ Electrotechnical Faculty, Belgrade University, Yugoslavia

Received 22 August 1995, in final form 9 April 1996

Abstract. Electron transport properties of single-crystal GaAs were determined using the photoacoustic method with the transmission detection configuration. The excess-carrier lifetime, the front and the rear recombination velocity, and the coefficients of the carrier diffusion and the thermal diffusivity were determined by comparing experimental results and theoretical photoacoustic signals.

1. Introduction

Photoacoustic (PA) methods have been extensively developed during the last ten years [1, 2, 3]. Rosencwaig and Gersho [4, 5] introduced PA spectroscopy and the first theoretical explanation based on the thermal piston model. Miranda [6], Sablikov and Sandomirski [7] and Vasilev and Sandomirski [8] extended the model with the effects of nonradiative volume and surface recombination of photogenerated carriers, including the effect of diffusion. More recently Pinto Neto *et al* studied the PA effect in PbTe, Si [9] and GaAs [10] in a transmission detection configuration which they called the open photoacoustic cell (OPC).

In this paper we have carried out an investigation of transport and thermal properties at room temperature of single-crystal GaAs using the frequency PA method with the transmission detection configuration.

2. Experimental results

PA amplitude and phase spectra were measured using a specially constructed PA cell [11] whose construction was optimized to obtain maximal acoustical protection from the surrounding influences (figure 1). The result was the achievement of a good signal–noise ratio and a flat frequency characteristic in the range between 60 and 6000 Hz. Therefore, these alterations enabled the obtaining of high-quality PA amplitude and phase signals compared with those for similar previously published experimental arangements [10].

The PA signals were measured using an experimental set-up with a He–Ne laser (25 mW) as an optical source. The laser beam was modulated with a mechanical chopper and

0953-8984/96/305673+11$19.50

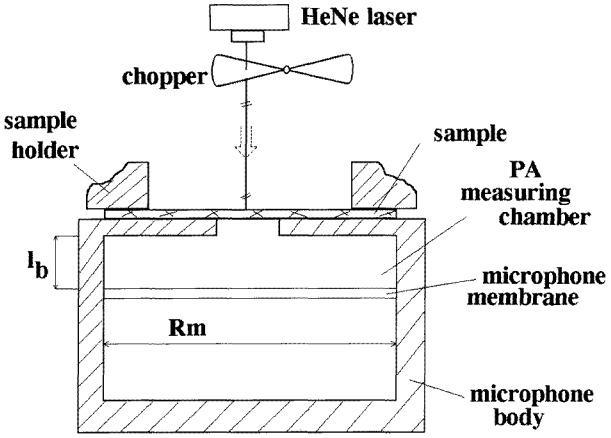

Figure 1. The gas–microphone PA cell with transmission detection (detail).

the sample was irradiated by a large spot (3 mm in diameter) in order to exclude the effect of lateral diffusion in the sample being studied. The measurements were made for a single-crystal n-type GaAs sample with orientation (100) and doped with Te atoms ($N_d \approx 10^{18}$ cm^{-3}). The sample was of a disc shape with a diameter of about 9 mm, and it was mounted directly on the front of an electret microphone which had a 3 mm diameter circular window as the sound inlet.

One side of the sample surface was polished using diamond paste of 6 μm grade, while the other side was roughened by polishing it with an abrasive silicon carbide P500 sandpaper. The measurement position was with the polished side in contact with the electret microphone and the roughened side illuminated by the laser beam.

In figure 2 the amplitude (a) and phase (b) PA signals, versus the modulation frequency, for six different sample thicknesses (1070 μm, 864 μm, 704 μm, 653 μm, 580 μm, 541 μm, 420 μm and 354 μm) are given.

3. Theoretical model

Following the Rosencwaig–Gersho thermal piston model [5], a complex system in the gas–sample–backing–microphone detection configuration given in figure 3 is considered, representing the PA cell in the transmission configuration, given in figure 1. The microphone detects the average pressure produced in the PA cell, whose volume is very small and in our case is $\pi R_m^2 l_b \approx 50$ mm^3, where R_m is the inner radius of the electret microphone, and l_b is the distance between the sample and the microphone membrane.

The theoretical treatment should quantitatively account for the amplitude and the phase of the PA signal and give their functional dependence on the modulation frequency. The light source is chosen to be a sinusoidally modulated monochromatic laser beam. Its intensity $I(x)$ at the depth x in the sample is

$$I(x) = (1 - R)\frac{I_0}{2}\,\mathrm{e}^{\alpha x} \tag{1}$$

where I_0 is the intensity of the laser beam; R is coefficient of reflectivity of the light beam from the surface, while α is the optical absorption coefficient.

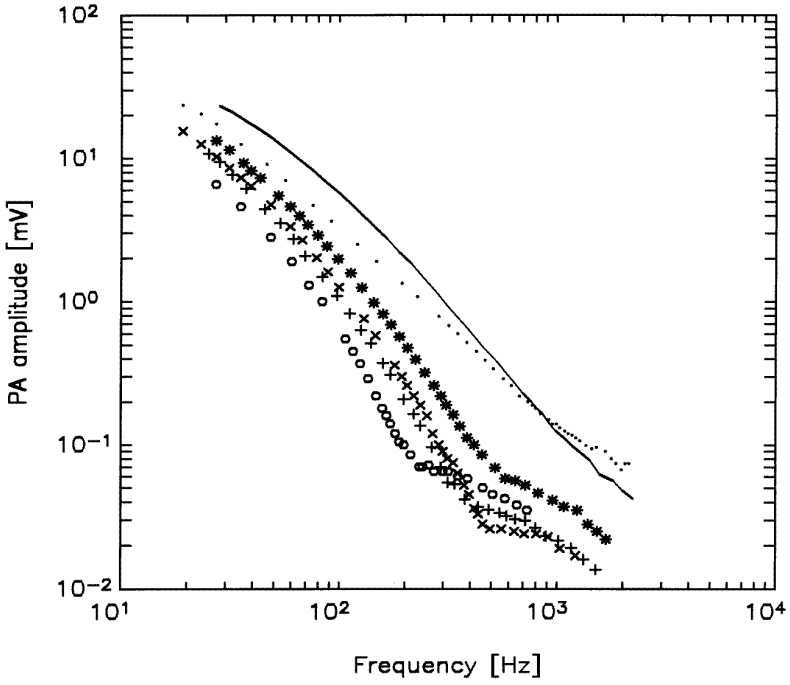

(a)

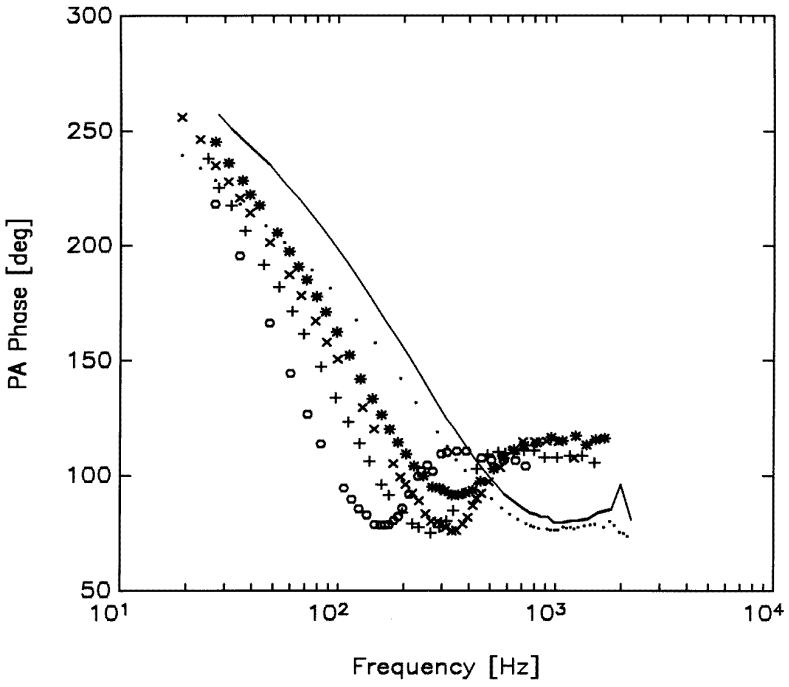

(b)

Figure 2. The amplitude (a) and phase (b) PA signals, versus the modulation frequency, for six different sample thicknesses: (○) 1070 μm; (+) 864 μm; (×) 704 μm; (⋆) 653 μm; (●) 420 μm; (——) 354 μm.

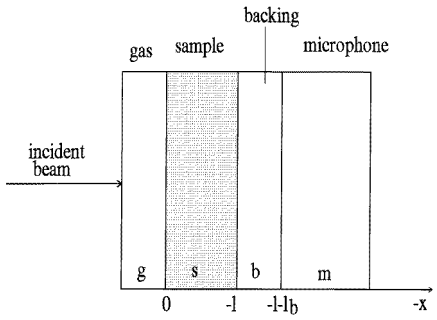

Figure 3. The cross-section of the PA cell with the transmission detection configuration.

Using the above-mentioned thermal piston model, the PA signal, $S_t(-l,\omega)$, should be a consequence of heat diffusion processes in the sample, i.e. it is a function of periodic temperature variation of the sample–backing (gas) surface, $\Phi(-l,\omega)$, and its thermodiffusion component can be given by the following equation:

$$S_t(-l,\omega) = \gamma \frac{P_0}{T_0} \frac{1}{k_b l_b} \Phi(-l,\omega) \tag{2}$$

where P_0 and T_0 are the ambient pressure and the room temperature, respectively; l_b is the distance between the sample and the microphone membranes, and γ is the adiabatic constant.

The index b indicates backing parameters. For the sake of simplicity the index s to indicate sample parameters was omitted. Also, shorthand notation will be used in further work. For example, $\Phi(-l,\omega)$ will be denoted as $\Phi(-l)$, etc.

Now we should take into account the density distribution of excess carriers and the temperature field. The influence of thermomechanical and electromechanical contributions can be neglected, and the diffusion equation, related to the density of excess carriers in GaAs, $\Delta n(x)$, can be expressed by the following equation:

$$\left(\frac{\mathrm{d}^2}{\mathrm{d}x^2} - \frac{1}{L_\omega^2}\right)\Delta n(x) = I_0(1-R)\frac{\alpha}{2ED}\mathrm{e}^{\alpha x} \tag{3}$$

where $L_\omega^2 = D\tau/(1+\mathrm{i}\omega\tau)$; $D \approx 2D_nD_p/(D_n+D_p)$ is the ambipolar diffusion coefficient of excess carriers, where D_n and D_p are the electron and hole diffusion coefficients, respectively; τ is the lifetime of the excess carriers, and E is the excitation energy. In our case (for GaAs with $E_g = 1.43$ eV and $N_d \approx 10^{18}$ cm^{-3}) the ambipolar diffusion coefficient is almost equal to the diffusion coefficient of minority carriers, and the excitation energy is much greater than the energy gap of the measured sample, E_g.

The solution of equation (3) is

$$\Delta n(x) = A_+ \exp(x/L_\omega) + A_- \exp(-x/L_\omega) + A_\alpha \exp(\alpha x) \tag{4}$$

where A_+, A_- and A_α are integration constants. These integration constants were obtained from the following boundary conditions:

$$D\frac{\mathrm{d}}{\mathrm{d}x}\Delta n(x)|_{x=0} = -s_g\,\Delta n(0) \tag{5}$$

$$D\frac{\mathrm{d}}{\mathrm{d}x}\Delta n(x)|_{x=-l} = s_b\,\Delta n(-l) \tag{6}$$

where s_g and s_b are the surface recombination on the front (illuminated) and rear sample surfaces, respectively. The analytical solutions for the integration constants A_+ and A_- are

$$A_\pm = \pm\frac{A_\alpha}{A_L}\left[(1\mp\sigma_g)(1-\delta\sigma_b)\exp(-\alpha l) - (1\pm\sigma_b)(1+\delta\sigma_g)\exp(\pm l/L_\omega)\right] \tag{7}$$

where

$$A_L = (1+\sigma_g)(1+\sigma_b)\exp(l/L_\omega) - (1-\sigma_g)(1-\sigma_b)\exp(-l/L_\omega)$$

and $\delta = \alpha L_\omega$; $\sigma_i = D/(s_i L_\omega)$ and $v_D = D/L_\omega$; also

$$A_\alpha = \frac{I_0(1-R)}{2E}\frac{\delta}{v_D(1-\delta^2)}.$$

For this theoretical model the density of excess carriers is supposed to be independent of frequency, at low frequencies where $\omega\tau \ll 1$. In that case their lifetime is so short that the free carriers recombine before the next photogenerating period is reached. At higher modulation frequencies $\omega\tau > 1$, the surface recombination has a much bigger influence where the surface recombination velocity, s_b, of the side nearer to the microphone has a larger effect than the front surface recombination velocity s_g.

The temperature distribution in the PA cell must be known for determining the amplitude and the phase of the PA signal. In our case, it is necessary to know the periodic component of the temperature distribution, $\Phi_i(x)$.

Therefore the following system of thermal diffusion equations should be solved:

$$\left(\frac{\mathrm{d}^2}{\mathrm{d}x^2} - {k_i}^2\right)\Phi_i(x) = \begin{cases} 0 & i = \mathrm{g, b} \\ -H(x) & i = \mathrm{s} \end{cases} \tag{8}$$

$$k_i = \sqrt{\frac{\mathrm{i}\omega}{2D_{Ti}}}.$$

Here k_i is the wave number of the thermal wave, D_{Ti} representing the thermal diffusivity of layer i, and $H(x)$ is the thermal source in the sample.

The thermal source has three components: the fast thermalization component $H^T(x)$; the slow bulk recombination component $H^{BR}(x)$; and the surface recombination H_i^{SR}.

The temperature distribution on the surface which is in contact with the electret microphone is

$$\Phi(-l) = \Phi^T(-l) + \Phi^{BR}(-l) + \Phi^{SR}(-l) \tag{9}$$

where $\Phi^T(-l)$ is the thermalization component, $\Phi^{BR}(-l)$ is the volume recombination component, and $\Phi^{SR}(-l)$ is the surface recombination component.

Now it is possible to calculate the PA signal as

$$S_t(\omega) = C_{tb}\left[\Phi^T(-l) + \Phi^{BR}(-l) + \Phi^{SR}(-l)\right] \tag{10}$$

where $C_{tb}(\omega) = \gamma P_0/(T_0 k_b l_b)$.

In our case $E \gg E_g$, $\mathrm{e}^{-\alpha l} \sim 0$ for the short-wavelength excitation optical source, and also we can neglect the heat flow into the surrounding gas. Thus, the variation of the temperature on the rear surface of the sample is

$$\Phi(-l) = \frac{I_0(1-R)}{2Kk}\gamma_R\frac{E-E_g}{E}\frac{\alpha^2}{k^2-\alpha^2} + \frac{E_g}{Kk}\frac{1}{\sinh(kl)}\left[s_g\,\Delta n(0) + s_b\,\Delta n(-l)\cosh(kl)\right]$$
$$- \frac{1}{\sinh(kl)}\left[gK_1 - K_2\sinh(kl) + K_3 + K_4\cosh(kl)\right] \tag{11}$$

where

$$K_1 = \gamma_R \frac{E_g}{K\tau} A_\alpha \left(\frac{A_+}{k^2 - 1/L_\omega^2} + \frac{A_-}{k^2 - 1/L_\omega^2} + \frac{1}{k^2 - \alpha^2} \right)$$

$$K_2 = -\gamma_R \frac{E_g}{K\tau} A_\alpha \left(\frac{A_+}{k^2 - 1/L_\omega^2} \exp(-l/L_\omega) + \frac{A_-}{k^2 - 1/L_\omega^2} \exp(l/L_\omega) \right)$$

$$K_3 = \chi\gamma_R \frac{E_g}{K\tau} A_\alpha \left(\frac{A_+}{k^2 - 1/L_\omega^2} - \frac{A_-}{k^2 - 1/L_\omega^2} + \frac{r}{\chi} \frac{1}{k^2 - \alpha^2} \right)$$

$$K_4 = -\chi\gamma_R \frac{E_g}{K\tau} A_\alpha \left(\frac{A_+}{k^2 - 1/L_\omega^2} \exp(-l/L_\omega) - \frac{A_-}{k^2 - 1/L_\omega^2} \exp(l/L_\omega) \right)$$

$$r = \frac{\alpha}{k} \qquad \chi = \frac{1}{kL_\omega}.$$

4. Discussion

There is a decrease in the electret microphone sensitivity in the frequency range below about 100 Hz, so the experimental amplitude and phase PA signals should be corrected in the modulation frequency range between 10 and 100 Hz. Thin aluminium tapes (between 25 and 65 μm thick) were used as a reference sample, and thus it is possible to make a reliable correction of PA amplitude diagrams for the GaAs sample. This procedure was previously explained elsewhere [11].

Then corrected experimental PA amplitude diagrams for GaAs were fitted in the frequency range below 100 Hz with the theoretically calculated PA signals. There the thermal diffusivity and optical absorption coefficient were used as fitting parameters. The next step was to correct the phase diagrams, for the same sample, using the same amplitude-fitting procedure.

In this paper we have used also another less complicated method of normalization. PA experimental diagrams for the same sample, but with two different thicknesses, were used. This normalization procedure is used to eliminate the influence of the measuring system, especially that of the electret microphone. The signal ratio for these two different thicknesses of the measured GaAs sample was calculated using the following equation:

$$\frac{S_1(\omega)}{S_2(\omega)} = \left| \frac{\Phi(-l_1)}{\Phi(-l_2)} \right| \exp\left[\mathrm{i}(\varphi_2(-l_1) - \varphi_2(-l_2)) \right] = A_n \mathrm{e}^{\mathrm{i}\,\Delta\varphi} \tag{12}$$

where A_n is the amplitude ratio and $\Delta\varphi$ is the phase difference of the experimentally measured PA signals for two different sample thicknesses.

The PA spectra of GaAs for eight sample thicknesses (1070 μm, 864 μm, 704 μm, 653 μm, 580 μm, 541 μm, 420 μm and 354 μm) were measured. The sample with the largest thickness was not analysed numerically, because in that case the PA amplitude was very small. For these measurements, the transmission detection configuration was used for the PA signal, and the signal for very thick samples was very small; so the signal/noise ratio is much worse, compared with the other cases. For thick samples the PA signal could also be measured in the narrow frequency range up to about 700 Hz, while for thinner samples the PA signal could be measured even at frequencies above 1500 Hz. The sample thickness of 541 μm was not suitable for numerical analysis because it was very near to 580 μm.

For our eight thicknesses of the GaAs sample we have produced four normalized PA amplitude and phase spectra; typical examples of the amplitude- and phase-fitted diagrams are given in figures 4(a) and 4(b), respectively, for the case of a sample 704 μm thick normalized with a sample 420 μm thick.

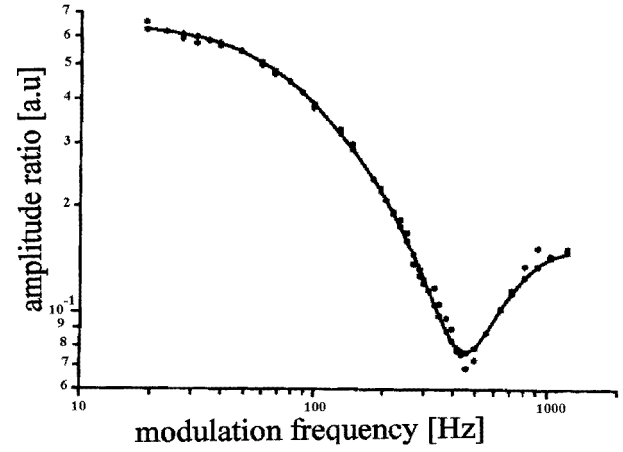

(a)

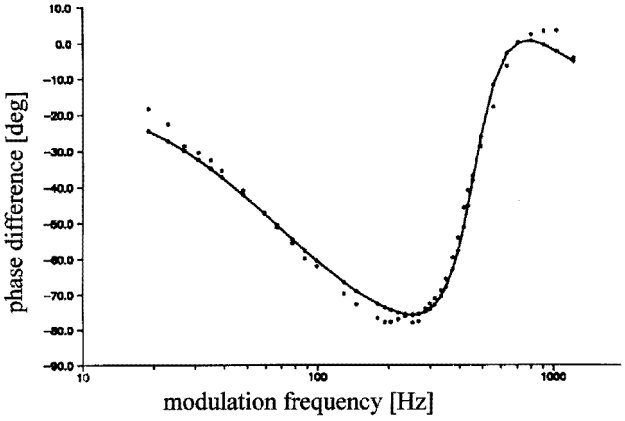

(b)

Figure 4. The normalized-amplitude (a) and normalized-phase (b) PA spectra for the GaAs sample (the thickness of 704 μm was normalized with a thickness of 420 μm): (●) experimental and (——) theoretically fitted spectra.

The fitting program was developed in the program language FORTRAN (MS-Fortran, version 5). This program enables the user to choose the values of parameters in the mathematical model. Practically all of the parameters used can be fitted. The user selects the magnitude of the change of each parameter. If some parameter should stay unaltered then the change of the parameter should be selected to be zero. One can simultaneously fit the amplitude and phase separately or both together. The fitting error can be estimated using one of the following criteria: (a) the sum of absolute differences between the experimental and the calculated values; (b) the sum of the squares of the differences between the calculated and the experimental values; (c) the sum of relative errors; and (d) the sum of the squares of the relative errors.

Therefore, the experimental curves can be compared with the theoretical one obtained from the mathematical model for the given parameters, and their values can be determined

during the fitting procedure. The value of the errors is shown after a limited number of iterations during the fitting procedure. In that way the user can follow the change of the errors and see whether the fitting procedure converges or not. Depending on this, the user can react (or not) in the following way: (a) to continue the fitting procedure if the error is continuing to decrease; or (b) to change the value of some parameters if the decrease of the error is extremely small (or if it does not change).

Table 1. The values of adjustable parameters obtained by the fitting procedure.

Ratio of thickness	τ (μs)	s_b (cm s^{-1})	s_g (cm s^{-1})	α (10^6 cm^{-1})	D_T (cm^2 s^{-1})
864/580	3.3	660	8922	0.5930	0.228
704/420	2.7	583	2643	0.7259	0.222
864/354	2.8	590	10 270	0.6342	0.230
678/420	2.8	570	9142	0.6066	0.224

Table 1 contains the values of the fitted parameters obtained by the fitting procedure for four normalized PA spectra. The values of the following parameters were calculated: excess-carrier lifetime (τ), front surface recombination velocity (s_g), rear surface recombination velocity (s_b), optical absorption coefficient (α) and thermal diffusivity coefficient (D_T).

From the analysis of the fitting procedure, using the criterion of the sum of the squares of the relative errors, the following accuracies of the fitted parameters were obtained: the excess-carrier lifetime (τ) within $\mp$2%; the front (s_g) and rear (s_b) surface recombination velocities within $\mp$10%; the optical absorption coefficient (α) within $\mp$5%; and thermal diffusivity coefficient (D_T) within $\mp$2%.

It is important to show how sensitively the fitted curves depend on the fitting parameters. To illustrate this figures 5(a) and 5(b) show the change of the amplitude and phase spectra when the best-fitted value of the excess-carrier lifetime is decreased by 10%. Figures 6(a) and 6(b) show the change of the amplitude and phase spectra when the best-fitted value of the thermal diffusivity (D_T) for the same sample is decreased by 10%. In this case the minimum is shifted towards lower frequencies and the difference between the theoretically calculated and the experimental diagrams becomes very apparent.

Table 2. Typical values for calculated parameters obtained in this work, and literature data [10].

Sample origin	Thickness (μm)	Doping concentration (cm^{-3})	D (cm^2 s^{-1})	τ (μs)	s_b (cm s^{-1})	s_g (cm s^{-1})	α (m^{-1})	D_T (cm^2 s^{-1})
Our samples	420	$n \approx 10^{18}$	4.3	2.7	583	2643	7259	0.224
	580	$n \approx 10^{18}$	4.3	3.3	660	8922	5930	0.232
Literature data [10]	(1) 583	5.2×10^{17}	9.1	6.05	580.7	—	—	0.38
	(2) 420	$\sim 10^{18}$	5.71	5.72	489	—	—	0.39

Our results can be compared only with the results given in the literature by Pinto Neto (see [10]), for n-type GaAs samples of almost identical quality. Typical values for the calculated parameters obtained in this paper and literature data are provided in table 2 together with the doping concentration N_d of the samples.

Comparing the results given in table 2, one can easily see that the main differences between the present and literature data are for thermal diffusivity. Our value for D_T was

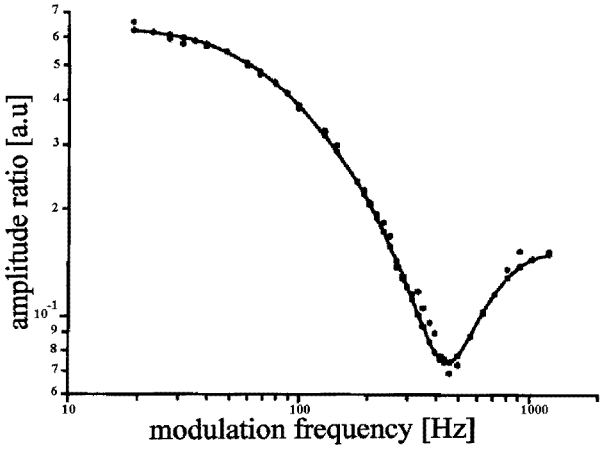

(a)

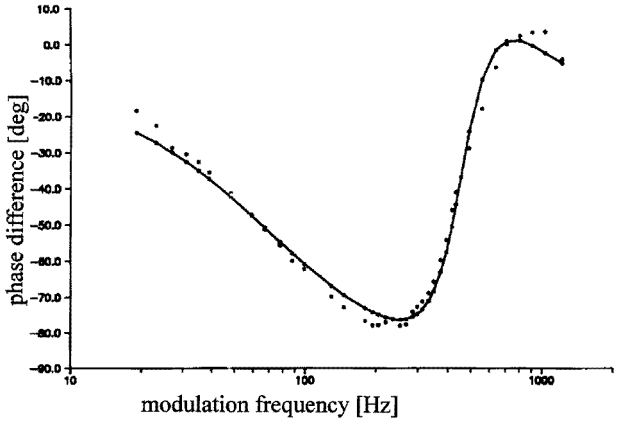

(b)

Figure 5. The change of the amplitude (a) and phase (b) diagrams for 704/420 μm normalized samples, when the best-fitted value of the excess-carrier lifetime is decreased by 10%.

about 0.23 cm^2 s^{-1} while the value in [10] was 0.39 cm^2 s^{-1}. The value for thermal diffusivity can be easily calculated provided that the thermal conductivity (K), density (ρ) and specific heat (C_P) are known, using the following relation:

$$D_T = \frac{K}{\rho C_P}. \tag{13}$$

In our case, for n-type GaAs with the carrier concentration $n = 10^{18}$ cm^{-3}, $K =$ 40 W m^{-1} K^{-1} [12]; the density $\rho =$ 5317.0 kg m^{-3} and the specific heat $C_P =$ 325 J kg^{-1} K^{-1} [13]. Then the calculated value for D_T is 0.231 cm^2 s^{-1}. This value is in reasonable agreement with our result obtained by the fitting procedure. It should be mentioned here that there are a variety of values for D_T in the literature. Our calculated value for D_T is in our opinion reliable for two reasons. First, our experimental results are very smooth, compared to the literature data [10], and have a much better signal/noise ratio. The second reason is that we have used a suitable theoretical model and fitting procedure.

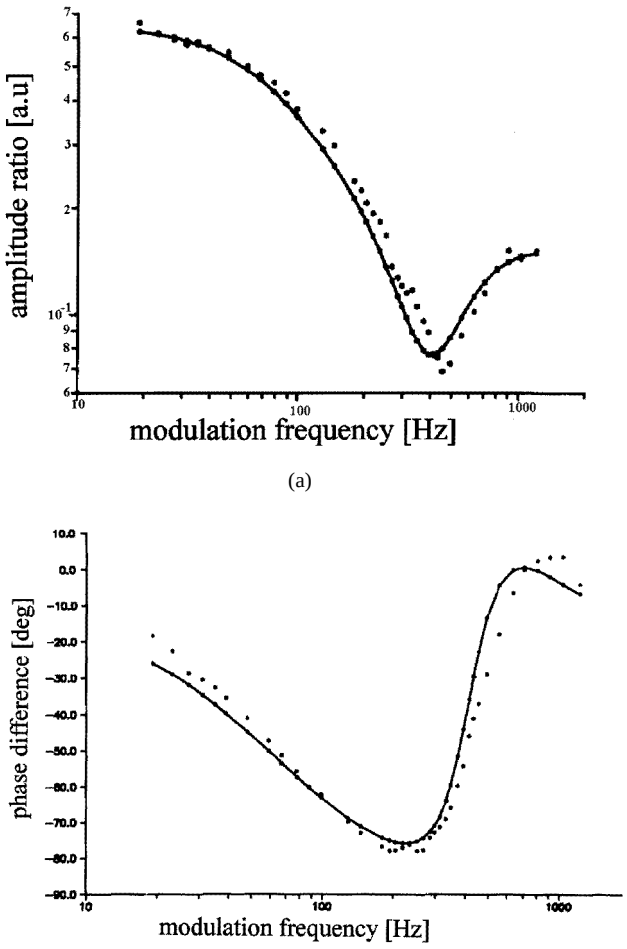

Figure 6. The change of the amplitude (a) and phase (b) diagrams for 704/420 μm normalized samples, when the best-fitted value of the thermal diffusivity is decreased by 10%.

5. Conclusion

In this paper we have made an investigation of thermal and electronic transport properties of single-crystal GaAs ($N_d = 10^{18}$ cm^{-3}) using a photoacoustic method with the transmission detection configuration. The values of the best-fitted parameters are: thermal diffusivity $D_T = 0.23$ cm^2 s^{-1}; excess-carrier lifetime $\tau = 3$ μs; recombination velocity of the polished sample surface about 580 cm s^{-1}; recombination velocity for the rougher side between 2600 cm s^{-1} and 10 270 cm s^{-1} (depending on the surface roughness); and the free-minority-carrier diffusivity $D = 4.3$ cm^2 s^{-1}).

Judging by how sensitively the fitted curves depend on the values of the fitting parameters, one can conclude that thermal diffusivity and electronic transport properties of semiconductors can be easily and quite accurately obtained using the PA frequency method with the transmission detection configuration.

References

[1] Mandelis A (ed) 1987 *Photoacoustic and Thermal Wave Phenomena in Semiconductors* (New York: North-Holland)
[2] Vargas H and Miranda L C M 1988 *Phys. Rep.* **161** 43
[3] Fournier D, Boccara A C, Skumanich A and Amer N M 1986 *J. Appl. Phys.* **59** 787
[4] Rosencwaig A 1973 *Opt. Commun.* **7** 305
[5] Rosencwaig A and Gersho A 1976 *J. Appl. Phys.* **47** 64
[6] Miranda L C M 1982 *Appl. Opt.* **21** 2923
[7] Sablikov V A and Sandomirski V B 1983 *Phys. Status Solidi* b **120**
[8] Vasilev A N and Sandomirski V B 1984 *Sov. Phys.–Semicond.* **18** 1095
[9] Pinto Neto A, Vargas H, Leite N and Miranda L C 1989 *Phys. Rev.* B **40** 3924
[10] Pinto Neto A, Vargas H, Leite N and Miranda L C 1990 *Phys. Rev.* B **41** 9971
[11] Nikolić P M, Todorović D M, Vasiljević D G, Mihajlović P, Ristovski Z, Elazar J and Blagojević V 1996 *J. Microelectron.* at press
[12] Baranski P I, Klockov V P and Potikevic I V 1975 *Poluprovodnikovaja Elektronika Svoistva Materialov* (Kiev: Naukova Dumka) pp 390, figure II 199
[13] EMIS 1986 Properties of GaAs *INSPEC Data Reviews, Series No 2* (London: Institution of Electrical Engineers)